ORIGINAL RESEARCH

Analyzing Thiol-Dependent Redox Networks in the Presence of Methylene Blue and Other Antimalarial Agents with RT-PCR-Supported in silico Modeling

J. Zirkel[1,3], A. Cecil[1], F. Schäfer[1,3], S. Rahlfs[2], A. Ouedraogo[3], K. Xiao[1], S. Sawadogo[3], B. Coulibaly[3], K. Becker[2] and T. Dandekar[1,4]

[1]Department of Bioinformatics, Biocenter, University of Würzburg, Germany. [2]Interdisciplinary Research Center, Justus Liebig University, Giessen, Germany. [3]Centre de Recherche en Santé de Nouna, Nouna, Burkina Faso. [4]European Molecular Biology Laboratory (EMBL), Heidelberg, Germany.
Corresponding author email: dandekar@biozentrum.uni-wuerzburg.de

Abstract

Background: In the face of growing resistance in malaria parasites to drugs, pharmacological combination therapies are important. There is accumulating evidence that methylene blue (MB) is an effective drug against malaria. Here we explore the biological effects of both MB alone and in combination therapy using modeling and experimental data.

Results: We built a model of the central metabolic pathways in *P. falciparum*. Metabolic flux modes and their changes under MB were calculated by integrating experimental data (RT-PCR data on mRNAs for redox enzymes) as constraints and results from the YANA software package for metabolic pathway calculations. Several different lines of MB attack on *Plasmodium* redox defense were identified by analysis of the network effects. Next, chloroquine resistance based on pfmdr/ and pfcrt transporters, as well as pyrimethamine/ sulfadoxine resistance (by mutations in DHF/DHPS), were modeled in silico. Further modeling shows that MB has a favorable synergism on antimalarial network effects with these commonly used antimalarial drugs.

Conclusions: Theoretical and experimental results support that methylene blue should, because of its resistance-breaking potential, be further tested as a key component in drug combination therapy efforts in holoendemic areas.

Keywords: methylene blue, resistance, drug, elementary mode analysis, malaria, combination therapy, pathway, metabolic flux

This article is available from http://www.la-press.com.

Background

Malaria treatment has had to cope with ever more resistant strains of *Plasmodium falciparum* and increasingly with straings of *Plasmodium vivax* as well. The spread of resistance to classical treatments triggered by widespread use of antibiotic such as chloroquine has led to a bleak situation and a rising disease burden since the 1980s, especially in Africa. Today malaria is responsible for around 5 billion clinical episodes resembling malaria, some 600 million clinical malaria cases, and about 1 million deaths due to malaria every year. The great majority of the malaria burden affects the poor, rural communities in sub-Saharan Africa (SSA), and most deaths occur in young children.[1–3] Economic instability and suboptimal medical treatment have led to a delicate situation and new strategies to fight malaria are urgently needed.[4–6] For decades chloroquine was the most important, safe, effective, and affordable antimalarial drug worldwide. The spread of chloroquine resistance was considered a public health disaster, and many countries adopted sulfadoxine-pyrimethamine (SP) as the first-line antimalarial treatment of choice.[2,4] In response to quickly spreading resistance to both chloroquine and SP, the World Health Organization (WHO) then recommended the use of combination treatments that include artemisinin derivatives as first-line therapy.[5]

Artemisinin-based combination therapies are the current first-line treatments of choice against malaria, though treatment costs are high and initial resistances have been reported in Southeast Asia.[7–12] Therapy costs of more than $5 per case are often unaffordable for the rural population most affected by malaria.[4,6,13–15] In this context, effective and cheap combination therapies are needed. Here we examine complementary aspects in order to introduce methylene blue (MB) combination therapies.

Methylene blue (MB), the first synthetic drug ever used against malaria[16] disappeared after other antimalarial drugs such as (eg, chloroquine) were introduced to the market in the 1960s. It was rediscovered some years ago[19,20] and it is currently being tested in phase IIb trials in Burkina Faso.[21] Previous studies could show that under treatment with MB, no serious adverse advents occurred; the most frequent side effects of MB were blue urine, vomiting and dysuria.[22] MB treatment is well received in the local population. However, in order to understand the antimalarial effects and appreciate the full potential of MB, a more detailed analysis of its biochemical effects is important.

MB is a subversive substrate and specific inhibitor of *P. falciparum* glutathione reductase. It inhibits heme polymerization within the parasite's food vacuole, and prevents methemoglobinemia in clinical malaria.[17,18] MB serves as a "*bon*aria" ("bon", beneficial, "a" affordable, "r" registered for methemoglobinemia, "ia" internationally affordable, as opposed to "*mal*aria") drug[19] with good combination potential for the treatment.[20,22–27] Here we consider some key aspects of such an MB-based strategy: resistance potential against standard drugs, model predictions and measurements of specific additive pathways, and anti-resistance effects of MB. In the context of increasing resistance and expensive antimalarial drugs such as artemisinin,[10–12] MB has several advantages—it is cheap, stable, and available.[20] MB inhibits the maturation of the parasite to the schizont stage by attacking multiple targets in *P. falciparum*, of which two, methemoglobin and β-hematin, are metabolites that are not controllable by the genome of the parasite, making resistance development against MB unlikely.[28] MB inhibits *P. falciparum* heme detoxification, and we show that it has a gametocytocidal effect on old and young gametocytes.[27] It is a subversive substrate and specific inhibitor of *P. falciparum* disulfide reductases such as the redox protein glutathione reductase (GR).[29] GR plays a key role in antioxidative defense systems and has been the subject of numerous investigations and reviews.[18,30,31]

We use here a combination of bioinformatics modeling and direct experimental tests to investigate the use of methylene blue in situations of resistance. First we give detailed data on the pleiotropic effect of methylene blue on redox pathways and redox protection. It has such an effect on *Plasmodium* spp., in particular on redox pathways, as shown here by pathway calculations (extreme pathway analysis) of experimental RT-PCR data on mRNAs for redox enzymes.

We used the YANA software package[32] to establish central metabolic pathways and calculate a metabolic flux model for *P. falciparum* capable of simulating the basic functions of the malaria parasite. The extreme pathway analysis is used to calculate the possible metabolic pathways in a given organism; the real-time PCR

data are used as constraints to identify the strength of the pathway fluxes under influence of MB. Next, we show that typical resistance mechanisms of malaria parasites against chloroquine or sulfadoxine affect pathways differently from those upon which MB is acting. We compare in silico the different modes of resistance in malaria, analyzing both chloroquine resistance based on pfmdr and pfcrt transporters and pyrimethamine/sulfadoxine resistance due to mutations in DHF and DHPS. Additionally, the effects of methylene blue on resistant and non-resistant *Plasmodium* strains are modeled.

Taken together, our data support the concept that MB could become a key component in new antimalarial combination therapies.

Materials and Methods
Preparation of parasite cDNA for transcriptome studies
In order to assess mRNA levels of parasites after MB treatment, *P. falciparum* trophozoites of the strain 3D7 were exposed to 15 nM of MB, which corresponds to approximately $5 \times IC_{50}$. After periods of 9, 12, and 18 hours, the parasites of the treated and untreated control plates were harvested by suspending the red cells for 10 minutes at 37 °C in a 20-fold volume of saponin containing red blood cell lysis buffer composed of 7 mM K_2HPO_4, 1 mM NaH_2PO_4, 11 mM $NaHCO_3$, 58 mM KCl, 56 mM NaCl, 1 mM $MgCl_2$, 14 mM glucose, and 0.02% saponin, pH 7.4. The suspension was centrifuged (1,500 g, 5 min, room temperature, for all steps), and the supernatant was discarded. Parasites were washed again in the above saponin buffer and finally in PBS. The parasite pellet was frozen in liquid nitrogen and kept at −80 °C. Disruption of parasites was achieved by freezing and thawing in liquid nitrogen three times. For extracting total RNA, the NucleoSpin RNA/Protein Kit (Macherey-Nagel, Düren, Germany) was used. RNA extracts were treated with concentrated DNase I (RNase-free; MBI Fermentas, St. Leon-Rot, Germany) according to the manufacturer's instructions for removing genomic parasite DNA contaminants confirmed by PCR. Aliquots of 450 ng RNA of each sample were reverse transcribed to cDNA using anchored oligo-dT primers (Reverse-iT MAX 1st Strand Synthesis Kit, Abgene, Hamburg, Germany).

Quantitative real-time PCR
The SYBR Green JumpStart Taq ReadyMix (Sigma-Aldrich) was used in the real-time PCR approach on a Rotor-Gene 3000 real-time PCR cycler (Corbett Research, Sydney, Australia). The required primers (Supplementary Table 1S) were designed in our laboratory. All primers used were tested previously in a normal PCR to ensure their target gene specificity. The Rotor-Gene 6.0 software was used to analyze the PCR results and to determine cycle threshold values. Data displayed are based on the threshold cycle and reaction efficiency of target and reference genes in both treated cells and untreated control cells. Relative quantification was carried out by applying the efficiency-corrected ΔCt method.[33] 18S rRNA was used as an internal reference gene. The specificity of PCR results was confirmed by melting curve analysis in which a negative control without a template was always included. In our experiments, each real-time PCR run was carried out in quadruplet. Standard errors are low and typically only 0.4% (one standard deviation); the actual ranges are given in Table 2 for each measured value.

Metabolic modeling
Calculation of all possible metabolic pathways
Extreme pathway (EP) calculation was used to evaluate the strain-specific redox network and central metabolism around folate synthesis, hemoglobin degradation, as well as porphyrin and carbon-pool networks in all contained pathways. A stoichiometric matrix (S: n*m) was prepared; the columns and rows correspond to the biochemical enzymes in the network (n) and the involved internal (produced or consumed within the network) metabolites (m), respectively. All of these internal metabolites have to be balanced. This is achieved by combining different enzymes so that in the end no internal metabolite accumulates or is depleted over time.

$$S\,v = 0 \qquad (1)$$

Calculation of pathway activities
Relying on a convex basis computation, a null-space matrix (**v**) capable of fulfilling the equation was calculated. The quality of the match to the actual measured gene expression values was calculated with the observed gene expression assumed to be proportional

to enzyme expression and taken as a direct estimate of the observed enzyme activity E_{obs}. This is of course an oversimplification since there are many additional factors and mechanisms regulating enzyme activities. Furthermore, this assumes that without gene expression data all core pathways are used equally (flux value = 1). The changes, particularly stronger or higher expression, were assumed to be proportional to the change in gene expression. However, these combined errors are greatly reduced by considering the complete network and the many available constraints according to the PCR-measured, significantly higher or lower gene expression data, and by including the available time-resolved data from transcriptome databases (eg, PlasmoDB).

Nevertheless, this metabolic modeling is not a detailed or meticulous modeling, considering all the individual kinetic constants and allosteric effects of different enzymes or, for instance, individual diffusion rates. However, it is sufficient enough (see results) to capture the network effects of different drugs and compare them. We ensured that convergence and low residual error for each metabolic model was obtained. This error was typically 0.6% of the enzyme activity calculated, the low value results as the complete network combines a number of constraints from the data; detailed results and convergence behavior for the calculations are given in Additional File 3. Standard errors are given in all figures.

First, each enzyme activity E_{pred} was calculated summing over the predicted activity A of each extreme pathway A_i containing this specific enzyme in its extreme pathway:

$$E_{pred} = \Sigma\, A_i \qquad (2)$$

Next, for the complete system of enzymes with significant gene expression changes, the squared deviation between predicted enzyme activity and observed enzyme activity, as estimated according to the gene expression data, was minimized:

$$\text{Min} \left(\Sigma\, (E_{pred} - E_{obs})^2 \right) \qquad (3)$$

This least-squares error minimization task can be achieved via different strategies. For best results in this minimization, we first used the genetic algorithm in YANAsquare and then a steepest descent routine written in R (see supplementary materials).

Results

The bioinformatics analysis on the redox network effects of methylene blue (MB) or other antimalarial drugs, alone or in combination and compared in wild type and resistant mutations, was obtained step by step, refining the analysis results by including more experimental data (our own or public) in each step. The workflow is given in Figure 1. After a first iteration to model all pathways, the results obtained were refined and analyzed further in detail as given in the following.

Modeling of all pathways
Pathways of the central and redox metabolic networks
In order to set up the central metabolism of *P. falciparum* with a focus on redox metabolism for building a network model, we used the database KEGG (http://www.genome.ad.jp/kegg)[34] and complemented the enzyme data produced by using sequence analysis, expert knowledge, and literature.[35] The software package YANAsquare[32] provides a database import tool, the KEGG Browser. This tool was used to import pathways of the central metabolism of *P. falciparum* from the KEGG database.[34] In order to achieve maximum model accuracy, proteins escaping previous annotation by KEGG were added to the preliminary pathway setup via sequence analysis and by incorporating data from PlasmoDB.[36] The stoichiometric validity of the enzymatic reactions considered was checked according to literature,[35] and the stoichiometric matrix of all enzyme reactions in the network was established (Additional File 1, Table S1). The set of all possible pathways that cannot be dissected any further was then calculated. These are the so-called elementary modes (see Materials and Methods). These show all metabolic pathways accessible for the system. Figure 2 summarizes the obtained network.

Fluxes
In order to model all pathways of the system, the convex basis vectors[37,38] of the flux distribution were calculated applying YANA.[32] After calculating the set of all potential pathways, it was important to determine actual fluxes for different pathways in the model. For this we used expression data from PlasmoDB[36] and the malaria transcriptome database (http://malaria.ucsf.edu/)[39] regarding the MB
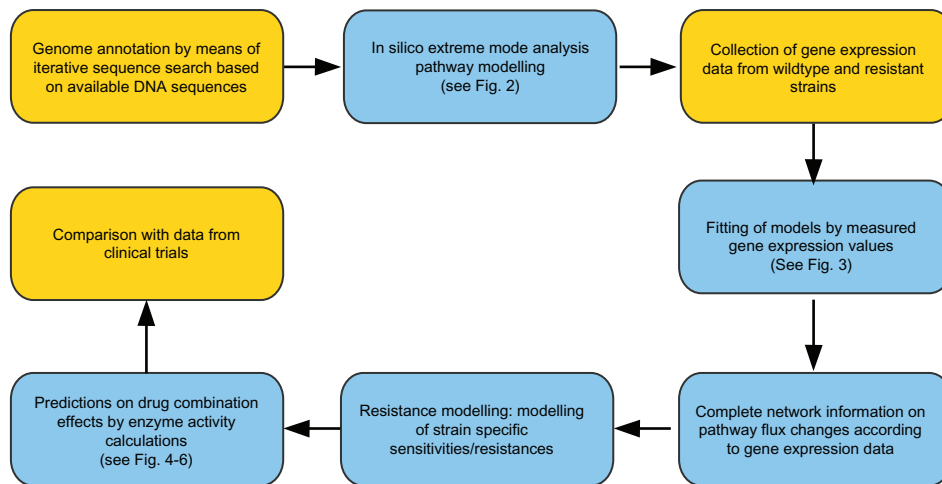
Figure 1. Workflow.
Notes: The following figures are indicated in the work flow scheme; supplementary data give detailed information on each step. Key experimental data are indicated in brown: (i) Genome annotation uses sequence analysis of the available data on the DNA sequence to identify all strain-specific enzymes and compare them to standard enzyme and pathway data from KEGG database. New predicted reading frames are verified by PCR. (ii) Central metabolic network with redox enzymes is set up accordingly, and all available pathways are calculated (solving the stochiometric matrix by elementary mode calculation). (iii) Model refinement by fitting the gene expression data to the measured enzyme activities to (iv) describe how pathways and metabolic flow change under different conditions (infected/uninfected and over time). (v) For resistance modeling, the enzyme activities for resistant/sensitive strains are altered according to antibiotic sensitivity using further gene expression data as constraints. (vi) Predictions on drug combination effects by means of enzyme activity comparisons between sensitive and resistant strains are compared with available public clinical data.

free situation. The latter database contains a relative mRNA abundance for every hour of the intra-erythrocytic cycle of parasite development based on a 70-mer oligonucleotide microarray. Next, enzyme expression values and relative changes in the MB treatment situation were estimated according to RT-PCR results (Table 2). These enzyme activities were first-order (ie, ignoring allosteric regulation) approximated by applying YANA and R[40] according to the best fit for the distribution of the flux modes for the given expression data (Fig. 3). Enzymes catalyzing more than one reaction were considered with each reaction modeled independently in order to obtain a more accurate calculation for enzyme activity and convex base mode calculations (eg, glutaredoxin reactions 1 through 6).

Modeling resistance mutations with and without MB

In order to calculate the effects of resistance against antimalarial drugs, we investigated different scenarios. For enzymes that were considered drug targets (in sensitive strains; see Figs. 4–6), we used PFCRT and PFMDR for chloroquine resistance, and DHF and DHPS for pyrimethamine/sulfadoxine resistance. The activity of the drug-targeted enzymes in a sensitive strain under drug influence

was defined to be zero but stayed normal for the resistant strains. All remaining enzyme activities were estimated according to the measured PCR-data as well as the malaria transcriptome database. Calculated fluxes were then fitted according to all these enzyme activity values. In this manner we created two clusters of 4 scenarios each (see Table 1, details for the calculated convex base pathway activities for all scenarios are given in Additional File 1, Tables 2S to 9S). For more detail on the workflow of these calculations, please refer to the subsection titled *YANAsquare short manual* in Additional File 2 (YANA_manual.doc). This gives an overview of the calculations and all results. Models are given in Additional File 3 (results.rar).

Inclusion of the PCR data: methylene blue acts in a pleiotropic manner on different redox enzymes

Methylene blue as a prooxidative agent increases oxidative stress on the parasite and has parasiticidal properties. We thus studied the actual pathway strengths under the influence of MB on such key enzymes of redox metabolism in *Plasmodium* spp. To obtain direct experimental data we conducted for this gene expression studies in cell culture (Table 2). Using RT-PCR, the gene expression changes after exposure to MB
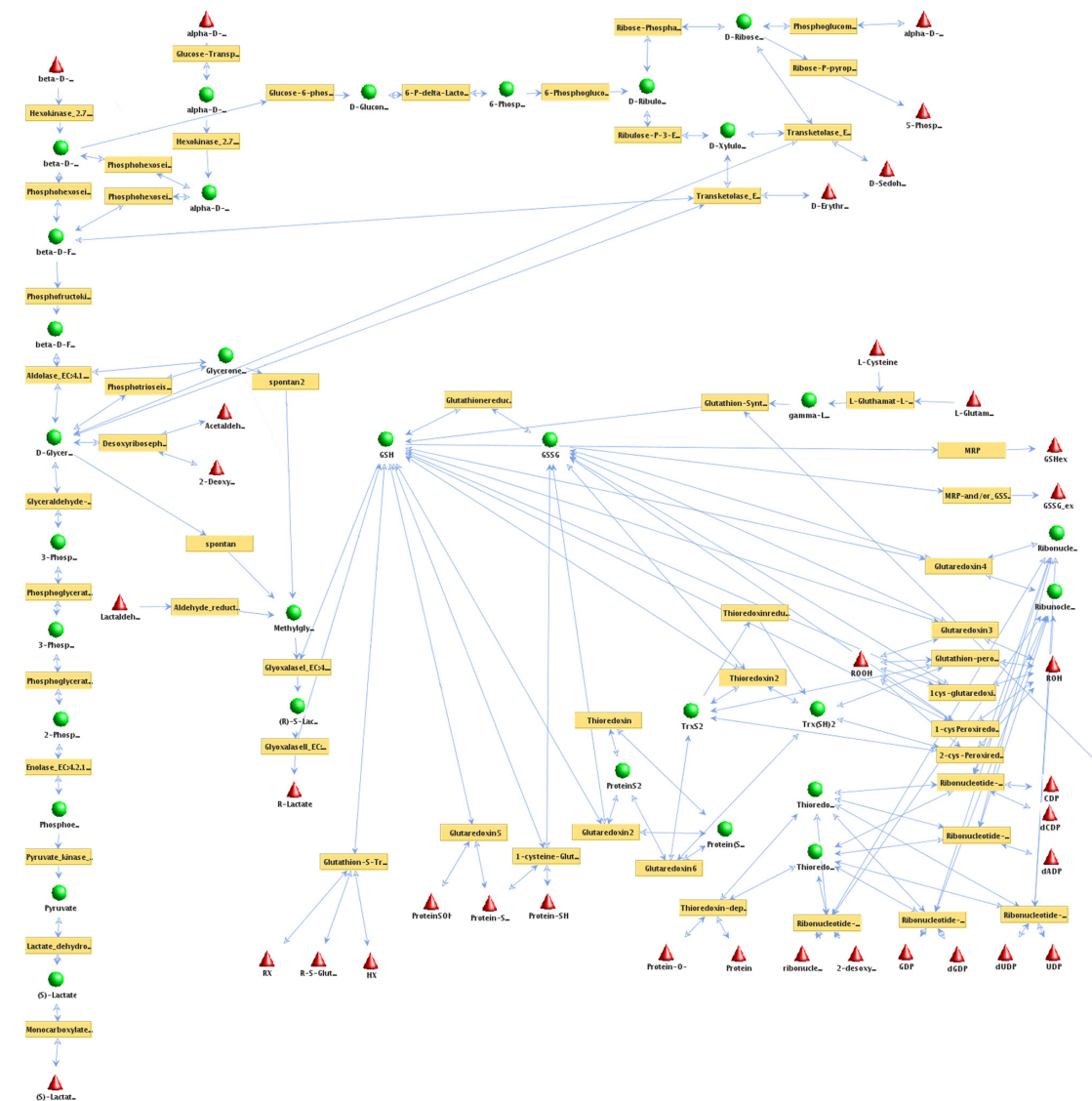
Figure 2. Pathways of plasmodial redox metabolism.
Notes: All accessible pathways of the redox network from *Plasmodium* spp were calculated applying elementary mode analysis (software: YANA). Enzyme names are written in brown boxes. A metabolite (names in black) is either a substrate or a product of a metabolic reaction. External metabolites (red triangles): metabolite is either taken up from the environment (substrate) or constitutes the end product of an enzymatic reaction. These are the sources or drains of the metabolic fluxes modeled and hence need not be balanced. Internal metabolite (green balls): metabolite concentration has to satisfy the steady state condition of the model as it is produced to cover the need of reactions using it in turn again as a substrate. Each of these internal metabolites has to be balanced by the enzymatic reactions of the metabolic network. All pathways are shown as equally active (blue arrows indicate fluxes) as this calculation indicates only which pathways could be used at all. To avoid cluttering of the picture, some connections to external metabolites are not shown. For full detail on all enzymes, substrates and fluxes calculated see Additional files. No transcription data or experimental mRNA expression data were incorporated at this stage.

were studied in correlation to a standard transcript. As the standard, we employed 18SRNA, which was found to be very stable over the incubation period. For all redox-associated proteins studied, transcript levels were downregulated after 9 hours. However GR expression strongly increased after 12 hours and marginally decreased again 18 hours later. GR as well as 1-Cys-peroxiredoxin and lactate dehydrogenase expression levels were enhanced after 18 hours.

Refined view on redox pathways affected by MB

Taking the PCR data into account, the MB-induced enzyme changes were modeled and further analyzed. mRNA activities for key redox enzymes were measured. A bioinformatics flux model calculated all fluxes as well as their changes in the whole network. Figure 3 summarizes the result obtained; thicker arrows represent strong pathway fluxes (Additional
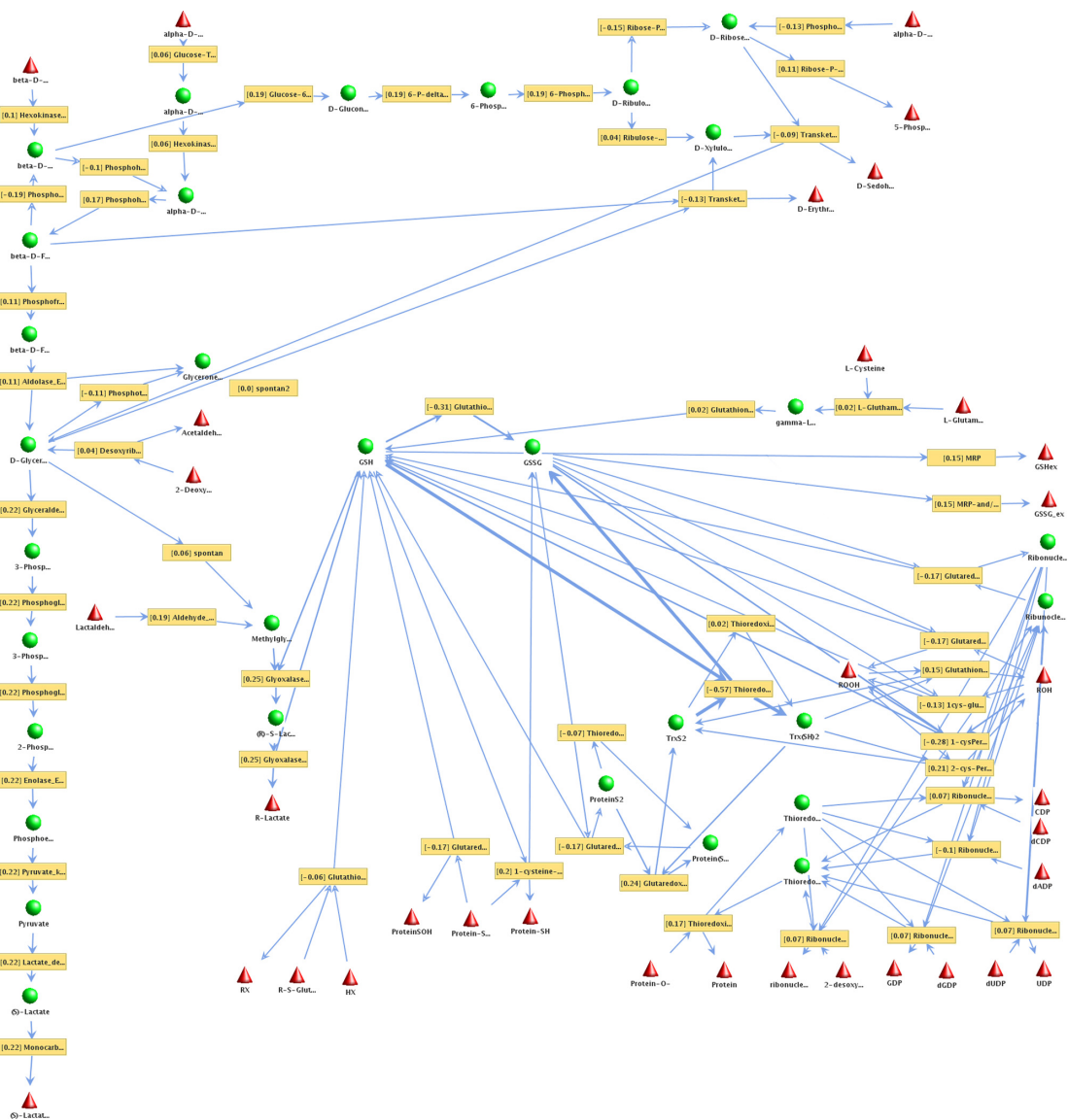
Figure 3. Changes in the *Plasmodium falciparum* redox flux network after MB drug action.
Notes: Results incorporating the transcription data and experimental mRNA expression data nine hours after incubation with methylene blue are shown. External metabolites are shown as red triangles, internal metabolites as green balls (see above). Enzyme names are written in brown boxes. Thicker arrows represent a stronger pathway flux. With methylene blue there is a shift in redox protection including glutathione reductase. Fluxes change according to utilization of the different pathways in the actual experiment and as a result of MB drug action (thinner and thicker arrows). To avoid cluttering of the picture, some connections to external metabolites are not shown. For full detail on all enzymes, substrates and fluxes calculated see Additional files.

file 1, Table 1S lists all involved enzymes; Additional file 2 results give all details on the flux mode calculations). YANAsquare estimated an overall flux distribution according to overall expression data from PlasmoDB[36] and the malaria transcriptome database. Changes were calculated using the gene expression changes of the key enzymes measured under different conditions as constraints. Though an individual gene expression change is only a rough and indirect estimate of the actual enzyme activity—factors such as translation, protein turnover and enzyme activation

are not captured—usage of all measured values as constraints helps to reduce the overall fitting error (remaining error: only few percent, see Liang et al[32] and Cecil et al[41]).

Without MB, 25 hours after invasion into the human erythrocyte, when the developmental stage of *Plasmodium falciparum* is the rapidly growing trophozoite, we found comparatively strong pathway fluxes (defined as relative changes > 0.15) in the following modes: protein protection (mode 2, 3, 6, 7, 11, and 35), generation of keto sugars (mode 18 and 23),
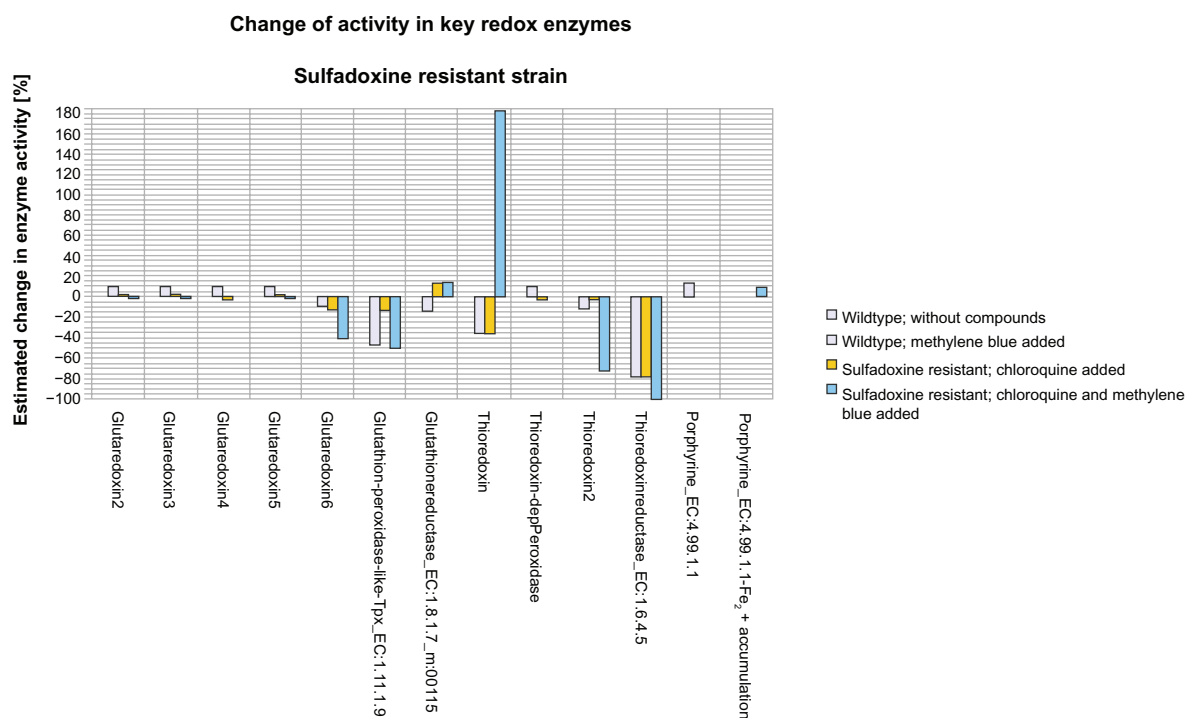
Change of activity in key redox enzymes

Sulfadoxine resistant strain

Figure 4. Changes in key redox enzymes—sulfadoxine-resistant strain.
Notes: Shown are the effects of chloroquine on key redox enzymes in a sulfadoxine-resistant plasmodium strain (yellow bar). The y-axis denotes estimated changes in enzyme activity in percent, the x-axis compares key redox enzymes. Also shown are the effects of a combination of chloroquine and methylene blue (blue bars) as well as the effects of MB on a non-resistant strain (grayish blue bar). As a baseline, the enzyme activities of a non-resistant strain without any added compounds were taken. Residual standard errors (from the percentage calculations, and given in %) after calculating the pathway activities were as follows (not drawn as these are quite small errors): wild type: 0.53, wild type and added MB: 0.54, chloroquine added: 0.68, chloroquine and MB added: 1.76.
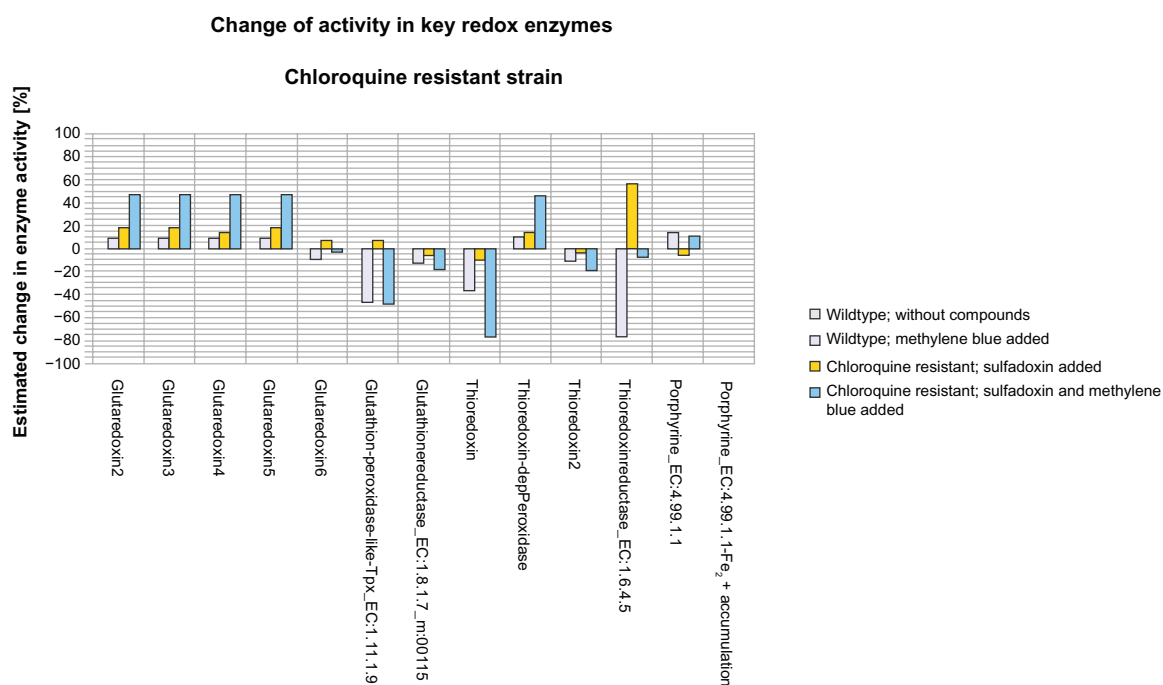
Change of activity in key redox enzymes

Chloroquine resistant strain

Figure 5. Changes in key redox enzymes—chloroquine-resistant strain.
Notes: Shown are the effects of sulfadoxine on key redox enzymes in a chloroquine-resistant plasmodium strain (yellow bar). The y-axis denotes estimated changes in enzyme activity in percent, the x-axis compares key redox enzymes. Also shown are the effects of a combination of sulfadoxine and methylene blue (blue bars), as well as the effects of MB on a non-resistant strain (grayish blue bar). As a baseline, the enzyme activities of a non-resistant strain without any added compounds were taken. Standard deviations (see Fig. 4 legend) after calculating the pathway activities were as follows: wild type: 0.53; wild type and added MB: 0.54; sulfadoxine-pyrimethamine and chloroquine added: 0.68; sulfadoxine-pyrimethamine, chloroquine, and MB added: 0.66.
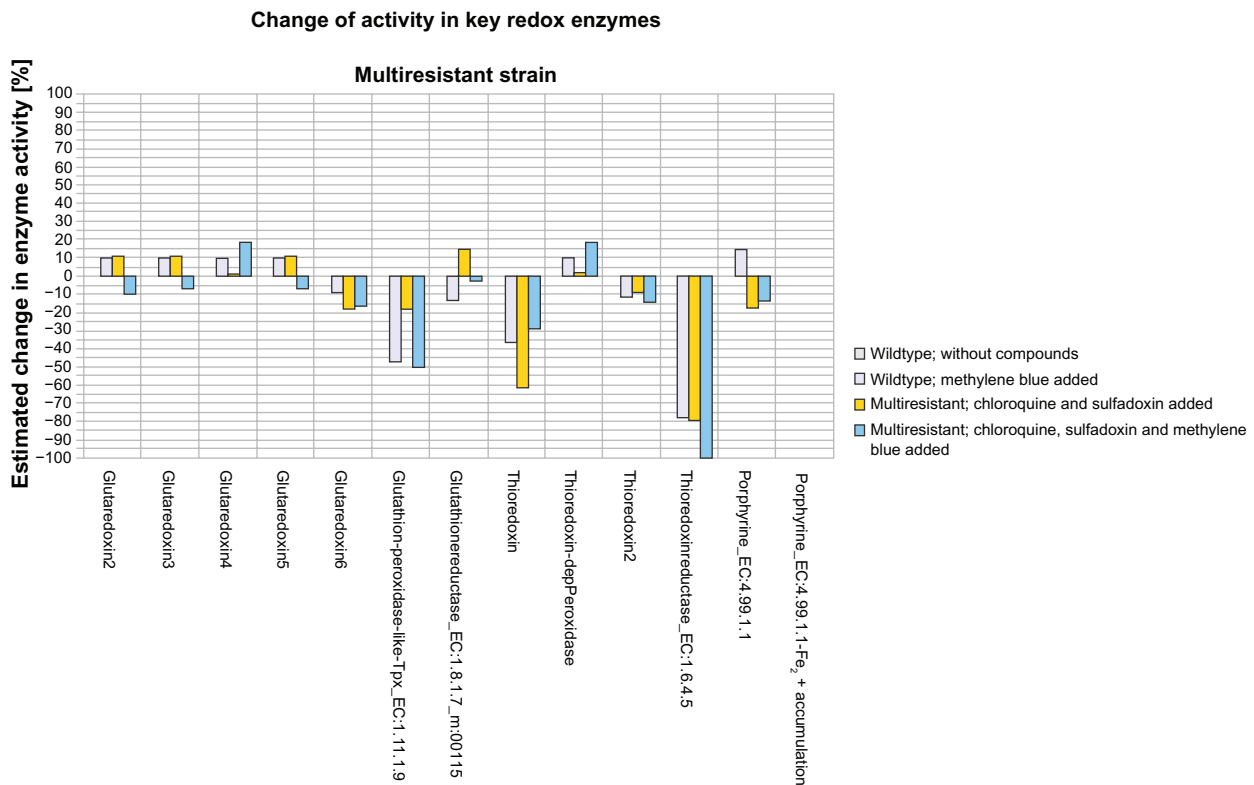
Change of activity in key redox enzymes

Figure 6. Changes in key redox enzymes—multi-resistant strain.
Notes: Shown here are the effects of the combination of the drugs chloroquine and sulfadoxine on key redox enzymes in a multi-resistant plasmodium strain tolerating via its resistance to both chloroquine and the administration of the drug sulfadoxine (yellow bar). The y-axis denotes estimated changes in enzyme activity in percent, the x-axis compares key redox enzymes. For comparison, we show the effects of a triple combination of chloroquine, sulfadoxine, and methylene blue (blue bars) as well as the effects of MB on a non-resistant strain (grayish blue bar). As a baseline, the enzyme activities of a non-resistant strain without any added compounds were taken. Standard deviations (see Fig. 4 legend) after calculating the pathway activities were as follows: wild type: 0.53, wild type and added MB: 0.54, sulfadoxine-pyrimethamine added: 1.75, sulfadoxine-pyrimethamine and MB added: 1.76.

and lactate production (mode 26). We conclude that the parasite spends its main activity on these metabolic processes and that these pathways play an important role for *Plasmodium* survival and growth in the host.

In the experiments conducted, the administration of MB slowed down all enzymes participating in these processes. Glutathione reductase showed that after an initial down regulation at 9 hours, an up regulation to 149% occured after 12 hours, which declined slightly after 18 hours (Table 2). Additionally, after 18 hours

under the chosen non-parasiticidal MB concentrations (15 nM), 1-Cys-peroxiredoxin and LDH showed, after initial down-regulation, an up-regulation of mRNA expression over the initial value.

The real-time PCR results were furthermore compared to the mRNA expression data of the DeRisi Database 25 hours after parasite invasion into the erythrocyte. In order to analyze the effects of methylene blue on the redox metabolism, we performed extreme pathway analyses and flux calculations with R.

Table 1. The different drug treatment scenarios.

Scenario	Enzyme activities according to drug resistance phenotype			
	#1	**#2**	**#3**	**#4**
1: without MB	Wild type strain, no resistance.	Chloroquine-resistant strain: Administration of sulfadoxine.	Sulfadoxine-resistant strain: Administration of chloroquine.	Strain resistant to chloroquine and sulfadoxine: Administration of chloroquine and sulfadoxine.
2: with MB added	Wild type strain, no resistance, MB administered.	Chloroquine-resistant strain: Administration of sulfadoxine and MB.	Sulfadoxine-resistant strain: Administration of chloroquine and MB.	Strain resistant to chloroquine and sulfadoxine: Administration of chloroquine, sulfadoxine, and MB.

Table 2. Gene expression differences under influence of methylene blue.

Protein	RT/18S		
	Relative mRNA expression after 9 h	Relative mRNA expression after 12 h	Relative mRNA expression after 18 h
Thioredoxin reductase	0.55 (±0.002)	0.74 (±0.003)	0.61 (±0.002)
Glutathione reductase	0.73 (±0.003)	1.49 (±0.006)	1.2 (±0.005)
Glyoxalase I	Not determined	0.51 (±0.002)	0.48 (±0.002)
Glyoxalase II	0.9 (±0.004)	0.36 (±0.002)	0.38 (±0.002)
Lactate dehydrogenase	0.7 (±0.003)	0.93 (±0.004)	1.93 (±0.008)
1-Cys-peroxiredoxin	0.59 (±0.002)	0.79 (±0.003)	1.27 (±0.005)
Glutaredoxin	0.88 (±0.004)	0.63 (±0.003)	0.7 (±0.003)
Glutamate-cysteine-ligase	0.61 (±0.002)	0.55 (±0.002)	0.54 (±0.002)
Thioredoxin-dependent peroxidase 1	0.45 (±0.002)	0.49 (±0.002)	0.39 (±0.002)
Glutaredoxin-like protein 1	0.51 (±0.002)	0.76 (±0.003)	0.66 (±0.003)

Under the influence of methylene blue (15 nM) after 12 hours, the protein protection modes 3, 6, 7, 11, and 22 were reduced by more than 4%. The strongest reductions (more than 10%) were calculated for protein protection modes 3, 6, 7, and 11, using thioredoxin and/or glutaredoxin. Ribose phosphate production for nucleotide metabolism was reduced by more than 17% in the most effected mode. The flux calculated for lactate generation was also reduced by 4%, whereas the generation of keto sugars remained nearly stable with minor fluctuations in the different modes (Table 12S). These results show that the parasite is subjected to more oxidative stress as the protein protection modes are more affected. Furthermore ribose phosphate production is reduced under these stress conditions. Consequently these effects are parasiticidal if lethal concentrations are used.

According to the calculated fluxes, the gene expression data for MB action on the parasite led to reduced protection against oxidative stress at multiple places in the network. Regarding the enzyme activity calculated under the influence of MB, we can show that enzymes participating in redox protection are less active and that the parasite is exposed to oxidative stress. For optimal activity (parasiticidal effect), a higher concentration (>20 nM) and/or longer incubation times (>18 hours) are required.

Modeling plasmodium resistance mutations and drug combinations

For detailed analysis of the resistance effects and drug combinations, we first simulated chloroquine-resistant *Plasmodium* parasites (PfCRT). We considered in particular the enzyme heme synthase as not susceptible to chloroquine (see Materials and Methods). In the chloroquine-resistant strain, hemozoin is formed by the oxidation of Fe^{2+} to Fe^{3+} and Fe^{3+} to protoporphyrin IX incorporated even in the presence of chloroquine.

Furthermore, the inhibition of dihydrofolate reductase (DHFR) and dihydropteroate synthase (DHPS) in a wild type strain was compared to plasmodial parasites resistant to such inhibition. In order to model the effects of these drugs on a sensitive strain in silico, we set the activities of drug-targeted enzymes to zero in order to simulate a best case scenario of complete sensitivity to the drug. For all enzymes that were not drug targets, we approximated their expression strengths, if available, by using the gene expression data.[39] Applying YANAsquare, we fitted the complete network fluxes for three resistance scenarios (see below) according to the data from the gene expression database or PlasmoDB.[36,39] Missing data were then calculated according to the total network fluxes, taking into account full or no activity for sensitive or resistant drug targets. Furthermore, for the scenarios with MB, the relative enzyme changes noted in the results section before were taken into account as a first-order estimate for MB action. Results were obtained for the following scenarios of drug combinations and different sensitivity or resistance of *Plasmodium*.

Scenario I
When chloroquine is acting alone on a sulfadoxine-resistant strain in comparison to a sensitive strain

(Fig. 4), the enzyme activity of glutaredoxin (main reaction: reaction 6), glutathione peroxidase-like thiol peroxidase (Tpx), thioredoxin, and thioredoxin reductase was lowered by at least 10%. Glutathione reductase increased its activity by 15%. In the case of thioredoxin there was a reduction of more than 30% and for thioredoxin reductase a reduction of more than 70% in enzyme activity. For the latter two enzymes, the effect was quite similar to that caused by administering MB alone. However, when additional MB was added to the chloroquine treatment, we could note several strong effects in some key redox enzymes; for example, thioredoxin reductase was completely inhibited by the MB/CQ combination. Thioredoxin was also influenced and the direction of the reaction changed while increasing two fold. This was also calculated for glutaredoxin (main reaction: reaction 6), although in that case activity decreased. The glutathione-dependent, peroxidase-like thiol peroxidase reduced its activity by more than 50%, whereas chloroquine alone reduced activity by only 13%. Thioredoxin 2 had a 73% loss in activity under MB/CQ combination.

When inhibited, no hemozoin could be formed, and Fe^{2+} accumulated in the cell. The in silico effects were modeled to be the same as in vitro and in vivo. This resulted in an accumulation of Fe^{2+} after the administration of chloroquine and the inhibition of ferrochelatase (EC 4.99.1.1). The modeling showed that redox pathways, especially the enzymes involved in protein protection against oxidative stress, are very active. Under the influence of chloroquine, thioredoxin reductase activity was inhibited, and mode 22 for protein protection was consequently less active (see Table 10S). Glutaredoxin, glutathione peroxidase-like Tpx, and thioredoxins 1 and 2 also had a loss in activity when chloroquine is added. The ferrochelatase only actively detoxified Fe^{2+} when no compound was added. Glutathione reductase became more active when chloroquine is added.

Scenario II

When sulfadoxine was added to a chloroquine-resistant strain (Fig. 5), we observed an increase in activity in glutaredoxin reactions 2, 3, 4, and 5, in thioredoxin-dependent peroxidase by 15%–18%, and 7% for glutaredoxin reaction 6 and for glutathione-peroxidase-like Tpx. Thioredoxin reductase showed

an increase of 56%. A decrease in enzyme activity was calculated for thioredoxin reaction 2, glutathione reductase, ferrochelatase, and thioredoxin 1 by up to 10%. When MB was added, we calculated a strong enhancement of these effects for glutaredoxin reactions 2, 3, 4, and 5, thioredoxin-dependent peroxidase, glutathione reductase, and thioredoxin 1 and 2. The activity of glutaredoxin reactions 2, 3, 4, and 5 and thioredoxin-dependent peroxidase was increased by nearly 45% (note that glutaredoxin reaction 4 changed its direction). Glutathione reductase showed a decrease in activity of 18%, as did thioredoxin 2. The activity of thioredoxin 1 decreased by 77% (with sulfadoxine alone only 10%). In this calculation, thioredoxin reductase showed an 8% decrease in activity, whereas it was more active under the influence of sulfadoxine alone (56%). Glutathione-peroxidase-like Tpx showed similar effects—with sulfadoxine there was a 7% increase in activity and with sulfadoxine/MB there was a 47% decrease.

In our model, resistance by MDR was also tested under the influence of chloroquine and sulfadoxine. For this condition, our model showed impaired activity for the glutaredoxins glutathione peroxidase-like thiol peroxidase, thioredoxin 1, and thioredoxin reductase. In contrast, the glutathione reductase shows higher activity.

Scenario III

When sulfadoxine and chloroquine were added to a multi-resistant strain (Fig. 6) resistant to both sulfadoxine and chloroquine so that key target enzyme activities for these two drugs do not change in spite of their administration (see Materials and Methods), an increase in activity of of 11% for glutaredoxin reactions 2, 3, and 5 and 14% for glutathione reductase was calculated. A decrease in activity by 17% was shown for glutaredoxin reaction 6, glutathione peroxidase-like thiol peroxidase, and ferrochelatase. There was a decrease of 9% for thioredoxin reaction 2, whereas thioredoxin reaction 1 was decreased by 61% and thioredoxin reductase by 80%. Methylene blue added to the sulfadoxine/chloroquine combination caused severe changes in nearly all key redox enzymes. Thioredoxin reductase was severely reduced. Thioredoxin-dependent peroxidase and glutaredoxin reaction 4 increased their activity by 18%, whereas the ferrochelatase was reduced by 13%.

In the case of glutaredoxin reactions 2, 3, 5, and 6, glutathione peroxidase-like thiol peroxidase, and thioredoxin reactions 1 and 2, the activity was reduced and the direction of reaction changed. This indicates a more severe effect on the parasite than the combination treatment alone.

As shown by metabolic flux modeling, the sulfadoxine-resistant strain showed an increased activity in glutaredoxin reactions 2, 3, 4, 5, and 6, glutathione peroxidase-like Tpx, thioredoxin-dependent peroxidase, and thioredoxin reductase, the latter especially so.

Discussion

As one of the oldest synthetic drugs used against malaria, MB was already successfully applied over 100 years ago for the treatment of this disease, even in children.[16,20,42,43] It was no longer used after other drugs (eg, chloroquine) were introduced to the market.

MB has been shown to selectively inhibit the *Plasmodium falciparum* glutathione reductase non-competitively. MB has the potential to reverse CQ resistance and it prevents the polymerization of heme into hemozoin, similar to the effect of 4-amino-quinoline antimalarials.[42,44] Previous studies investigated its synergy with CQ.[22,44] This combination was effective against malaria in most cases; however, chloroquine resistance has dramatically increased.[22,23,45] MB seems to be a slow-acting drug ($t_{1/2}$: ca. 5 hours), so a good partner drug should be a fast-acting one.[23] In a recent study MB (10 mg/kg) had a very strong gametocytocidal effect on *Plasmodium falciparum*.[25] This supports MB being used as a helpful drug for efforts in malaria eradication.

Despite repeated malaria infections, the parasite still escapes the immune system. Adults may acquire semi-immunity with mild disease symptoms. In young children the disease is life-threatening and malaria is the major reason for a childhood mortality rate of 35 per 1,000 per year.[45,46,48,49] No vaccine is currently available.[24] The best way to eliminate the holoendemicity is to break the life cycle of the parasite by impairing the vector, the blood stage parasites, or the gametocytes through a concerted, local effort for local eradication.[47] Specifically, the modeling and PCR data show that there is a multi-hit strategy evidenced by the MB effect; we see down-regulation of glutathione reductase protection and only some recovery. The same is true for the pathways of various protein protection modes, detoxification of 2-oxoaldehydes, generation and conversion of keto sugars, the lower part of glycolysis, and glutathione synthesis. The limits of estimates based on gene expression have been discussed previously.[26,41] In our model, multiple constraints lower the residual fitting error (to PCR data) for most fluxes to only a small percentage. Furthermore, the compensatory up-regulation of GR observed is likely to be counterproductive for the parasite, since MB is a subversive substrate turning the anti-oxidative glutathione reductase into a pro-oxidative enzyme. The broad and promising direct inhibitory effects of MB on parasite metabolism are consistent with clinical findings, where up to 95% of children suffering from malaria showed adequate clinical and parasitological response after MB treatment.[25]

We used a sub-lethal concentration in our experiments (15 nM for 18 hours corresponding to $5 \times IC_{50}$ determined after 72 hours) on purpose in order to monitor subsequent changes in gene expression that include parasite recovery. Direct drug effects on enzymes further improve the efficacy of methylene blue; the modes are additionally suppressed (eg, subversive substrate action on GR augments MB effect).

Furthermore, we use our estimates here only to underline the capabilities of MB, thus a semi-quantitative statement is appropriate. We can clearly show the trophozoiticidal effects of these via multiple direct hits on different enzymes by MB, including further redox pathway changes and impairment. We show here detailed results only for high but sub-lethal concentrations, but we also performed experiments with higher MB concentrations showing trophozoidal activity; the same trend of increasing inhibition for redox enzymes was witnessed including, at higher MB concentrations, more and more inhibition of glutathione reductase. The gametocytocidal effects of MB reported elsewhere[25] involve very similar pathways and can again be modeled with the same approach (future work). Resulting effects rely again on the multiple pathway hit strategy built into MB. Metabolic modeling of different drug resistance mechanisms done here point out that MB, due to its broad redox network pathway effects, can be well combined with different standard drugs used in malaria therapy.

This applies also to combination therapies such as BlueArte and BlueCQ, therapy with methylene blue and artemisinin or chloroquine, respectively. The different simulations detailed here show not only that because of resistant enzymes they differ to the wild type already in some fluxes but, more importantly, that different resistant strains become sensitive again when tackled by a combination therapy with MB.

Our data show that MB is a good drug for a combined attack on several pathways, in particular those involved in redox protection. It is thus an additional good candidate for drug combinations, as already suggested by previous work on the combination of MB with chloroquine or amodiaquine[23,25] or (see above) in combination with artemisinin. Furthermore, the combined attack on redox pathways by MB suggests it is a second-line drug to be given in addition to a first-line therapy when resistance is expected and breaking resistance is desired (see data above). The comparatively short half life of MB as a drug combines well and synergistically with other drugs with long half life (eg, choloroquine, amodiaquine) if given in suitable intervals.[23,25] This is critical for achieving an efficient combination of drug action, for instance when treating chloroquine-resistant malaria strains with a MB-chloroquine combination.

MB action is not impaired by the other drug resistance mechanisms investigated in our different scenarios. Even the MDR situation is not enough to successfully inhibit the action of MB on several different redox and metabolic pathways. Moreover, additional gene copies in these redox pathways are rare, and they can only partially affect the pleiotropic action of MB. Furthermore, unbalanced duplications would even lead to additional redox stress, for instance trisomia 21, where an additional chromosomal copy of peroxidase on chromosome 21 is not balanced by catalase, as this is found on another chromosome. Some genes' mRNA levels change relatively fast once chemical environments change. This is only to a certain extent true for the measured redox enzymes, as the comparison of our 9 hour data with the untreated control indicates. However, although we accurately measured here the 9 hour time point as the earliest time step after the untreated situation, a number of early and fast effects of MB are known regarding metabolic pathway effects. In particular, additional redox stress and disequilibrium builds up over time, starting from the initial blocking of redox enzymes such as glutathione reductase, which happens within minutes after administering MB.[20]

The models shown here are not only capable of performing those calculations for the different strains of *P. falciparum* 3D7. As shown in Figure 1, the process of preparing metabolic network models is highly modular; the enzymes comprising the metabolic pathways of *P. falciparum* 3D7 differ only slightly in other strains of *Plasmodium*. The pipeline (see Fig. 1) described in this work is easily and quickly transferable to other malaria strains for which the genome sequence is known. In particular, regarding *P. vivax*, the results are directly transferable in first approximation, as most enzymes modeled for *P. falciparum* by us also occur here. This is important since this *Plasmodium* strain is increasingly spread in tropical regions, and here the effect of the typical antimalarial drugs is not so well known including behavior in resistant strains.

MB is available on site in Burkina Faso as a *bonaria* drug (available, accessible, and registered) and has been studied here alone and in combination therapies. As a strong multi-target drug, it attacks the blood-stage parasite redox networks and other proteins, and it includes a very strong gametocytocidal effect as well. We suggest more investigations of MB and its effects on malaria eradication and recommend a combination therapy, since now there is no longer any single, 100% effective drug against the disease.[48]

In conclusion, administering a broad drug affecting multiple targets may become a general strategy to cope with resistance development in infections, including drug combination therapies. In the concrete case detailed here, these are various combinations of MB with first and second line antimalarial drugs to better treat malaria. The calculations of the detailed drug effects on redox networks strongly support the beneficial effects of MB combination therapies. They underscore that further clinical studies are promising as well as required in order to translate these bioinformatical insights into better antimalarial therapy in loco.

Acknowledgements

Funding

Competing Interests

Author(s) disclose no potential conflicts of interest.

Author Contributions

JZ, AC, and FS contributed equally to the work. Conducted bioinformatics analysis, modeling, and practical aspects of the study: JZ. Conducted bioinformatics and data analysis, modeling, extreme mode analysis: AC. Conducted data analysis, implementation aspects, anti-malaria strategies: FS. Conducted RT-PCR experiments: SR. Provided expert advice on the clinical treatment of malaria: AO. Provided assistance in genome and domain analysis: KX. Provided expert advice on in loco eradication efforts: SS. Provided expert advice on in loco treatment efforts and expertise for MB treatment: BC. Provided expert advice on all experimental aspects, redox and malaria: KB. Supervised JZ, AC, FS, and KX, lead and guided the study, and conducted analysis of the data: TD. Drafted the manuscript: AC, JZ, FS, BC, and TD. All authors were involved in reading and writing the manuscript and approved its final version.

Abbreviations

MB, methylene blue; Tpx, thiol peroxidase.

Disclosures and Ethics

The authors have provided signed confirmations to the publisher of their compliance with all applicable legal and ethical obligations in respect to declaration of conflicts of interest, funding, authorship and contributorship, and compliance with ethical requirements in respect to treatment of human and animal test subjects. Authors have confirmed that the published article is unique and not under consideration nor published by any other publication and that they have consent to reproduce any copyrighted material. The peer reviewers declared no conflicts of interest.

References

1. Greenwood BM, Bojang K, Whitty JM, Targett GA. Malaria. *Lancet*. 2005;365:1487–98.
2. Trape JF. The public health impact of chloroquine resistance in Africa. *Am J Trop Med Hyg*. 2001:12–7.
3. Trape JF, Pison G, Spiegel A, Enel C, Rogier C. Combating malaria in Africa. *Trends Parasitol*. 2002:2242–30.
4. Kouyaté B, Sie A, Yé M, De Allegri M, Müller O. The great failure of malaria control in Africa: a district perspective from Burkina Faso. *PloS Med*. 2007:127.
5. World Health Organization/UNICEF. *World Malaria Report* 2008. Available at: http://www.who.int/malaria/publications/atoz/9789241563697/en/index.html/.
6. Sachs JD. Achieving the millennium development goals—the case of malaria. *N Engl J Med*. 2005:115–7.
7. Osorio L, Gonzalez I, Olliaro P, Taylor WR. Artemisinin-based combination therapy for uncomplicated plasmodium falciparum malaria in Colombia. *Malar J*. 2007:25.
8. International Artemisinin Study Group. Artesunate combinations for treating uncomplicated malaria: a prospective individual patient data meta-analysis. *Lancet*. 2004:9–17.
9. Sutherland CJ, Ord R, Dunyo S, et al. Reduction of malaria transmission to anopheles mosquitoes with a six-dose regimen of co-artemether. *PLoS Med*. 2005:e92.
10. Duffy PE, Sibley CH. Are we loosing artemisinin combination therapy already? *Lancet*. 2005:1908–9.
11. Jambou R, Legrand E, Niang M, et al. Resistance of plasmodium falciparum field isolates to in-vitro artemether and point mutations of the SERCA-type PfATPase6. *Lancet*. 2005:1960–3.
12. Noedl H, Se Y, Schaecher K, Smith BL, Socheat D, Fukuda MM. Artemisinin resistance in Cambodia 1 (ARC1) study consortium. *N Engl J Med*. 2008:2619–20.
13. Bloland PB, Ettling M, Meek S. Combination therapy for malaria in Africa: hype or hope? *Bull World Health Organ*. 2000:1387–88.
14. Garner P, Graves PM. The benefits of artemisinin combination therapy for malaria extend beyond the individual patient. *PLoS Med*. 2005:e105.
15. Wiseman V, Kim M, Mutabingwa TK, Whitty CJM. Cost-effectiveness study of three antimalarial drug combinations in Tanzania. *PLoS Med*. 2006:e373.
16. Guttmann P, Ehrlich P. Über die wirkung des methylenblau bei malaria. *Berliner Klinische Wochenschrift*. 1891:953–6.
17. Coleman MD, Coleman NA. Drug-induced methaemoglobinaemia. Treatment issues. *Drug Saf*. 1996:394–405.
18. Buchholz K, Schirmer RH, Eubel JK, et al. Interactions of methylene blue with human disulfide reductases and their orthologues from plasmodium falciparum. *Antimicrob Agents Chemother*. 2008:183–91.
19. Schirmer RH. Medikamente für die Armen. *Spektrum der Wissenschaft*. 2004:110–3.
20. Schirmer RH, Coulibaly B, Schiek W, et al. Methylene blue in the treatment of malaria—past and presence. *Redox Report*. 2003:272–6.
21. Coulibaly B, Zoungrana A, Mockenhaupt FP, et al. Strong gametocytocidal effect of methylene blue-based combination therapy against falciparum malaria: a randomised controlled trial. *PLoS ONE*. 2009:e5318.
22. Meissner P, Mandi G, Coulibaly B, et al. Methylene blue for malaria in Africa: results from a dose-finding study in combination with chloroquine. *Malaria J*. 2006:84.
23. Mandi G, Witte S, Meissner P, et al. Safety of the combination of chloroquine and methylene blue in healthy adult men with g6PD deficiency from rural Burkina Faso. *Trop Med Int Health*. 2005:32–8.
24. Meissner P, Mandi G, Coulibaly B, et al. Methylene blue for malaria in Africa: results from a dose-finding study in combination with chloroquine. *Malaria J*. 2006:84.
25. Zoungrana A, Coulibaly B, Sié A, et al. Safety and efficacy of methylene blue combined with artesunate or amodiaquine for uncomplicated falciparum malaria: a randomized controlled trial from Burkina Faso. *PLoS One*. 2008:e1630.

26. Kilama W, Ntoumi F. Malaria: a research agenda for the eradication era. *Lancet*. 2009:1480–2.
27. Coulibaly B, Zoungrana A, Mockenhaupt FP, et al. Strong gametocytocidal effect of methylene blue-based combination therapy against falciparum malaria: a randomised controlled trial. *PLoS ONE*. 2009:5318.
28. Bozdech Z, Llinas M, Pulliam B, Wong E, Zhu J, DeRisi J. The transcriptome of the intraerythrocytic developmental cycle of plasmodium falciparum. *PLoS Biol*. 2003:5.
29. Atamna H, Krugliak M, Shalmiev G, Deharo E, Pescarmona G, Ginsburg H. Mode of anti malarial effect of methylene blue and some of its analogues on plasmodium falciparum in culture and their inhibition of P. vinckei petteri and P. yoelii nigeriensis in vivo. *Biochem Pharmacol*. 1996:693–700.
30. Schirmer RH, Coulibaly B, Stich A, et al. Methylene blue as an antimalarial agent. *Redox Rep*. 2003:272–6.
31. Vennerstrom JL, Makler MT, Angerhofer CK, Williams JA. Antimalarial dyes revisited: xan-thenes, azines, oxazines, and thiazines. *Antimicrob Agents Chemother*. 1995:2671–7.
32. Liang C, Liebeke M, Schwarz R, et al. Staphylococcus aureus physiological growth limitations: insights from flux calculations built on proteomics and external metabolite data. *Proteomics*. 2011:1915–35.
33. Pfaffl MW. A new mathematical model for relative quantification in real-time RT-PCR. *Nucleic Acids Res*. 2001:45.
34. Kanehisa M, Araki M, Goto S, et al. KEGG for linking genomes to life and the environment. *Nucleic Acids Res*. 2008:480–4.
35. Gerhard M. Biochemical pathways. Heidelberg, berlin: spektrum akademischer verlag GmbH; 1999:99–107.
36. Aurrecoechea C, Brestelli J, Brunk BP, et al. PlasmoDB: a functional genomic database for malaria parasites. *Nucleic Acids Res*. 2008:539–43.
37. Papin JA, Price ND, Palsson BO. Extreme pathway lengths and reaction participation in genome-scale metabolic networks. *Genome Research*. 2002:1889–900.
38. Larhlimi A, Bockmayr A. A new constraint-based description of the steady-state flux cone of metabolic networks. *Discrete Applied Mathematics*. 2009:2257–66.
39. Llinás M, Bozdech Z, Wong ED, Adai AT, DeRisi JL: Comparative whole genome transcriptome analysis of three plasmodium falciparum strains. *Nucleic Acids Research*. 2006:1166–73.
40. R Development Core Team. R: A language and environment for statistical computing. R foundation for statistical computing, Vienna, Austria 2006. Available at: http://www.r-project.org/.
41. Cecil A, Rikanović C, Ohlsen K, et al. Modeling antibiotic and cytotoxic effects of the dimeric isoquinoline IQ-143 on metabolism and its regulation in staphylococcus aureus, staphylococcus epidermidis and human cells. *Genome Biol*. 2011:24.
42. Schirmer RH, Coulibaly B, Stich A, et al. Methylene blue as an antimalarial agent. *Redox Rep*. 2003:272–6.
43. Vennerstrom JL, Makler MT, Angerhofer CK, Williams JA. Antimalarial dyes revisited: xanthenes, azines, oxazines, and thiazines. *Antimicrob Agents Chemother*. 1995:2671–7.
44. Krauth-Siegel RL, Bauer H, Schirmer RH. Dithiol proteins as guardians of the intracellular redox milieu in parasites: oldand new drug targets in trypanosomes and malaria-causing plasmodia. *Angew Chem Int Ed Engl*. 2005:690–715.
45. Becker K, Rahlfs S, Nickel C, Schirmer RH. Glutathione—functions and metabolism in the malarial parasite plasmodium falciparum. *Biol Chem*. 2003:551–66.
46. Becker K, Tilley L, Vennerstrom JL, Roberts D, Rogerson S, Ginsburg H. Oxidative stress in malaria parasite-infected erythrocytes: host-parasite interactions. *Int J Parasitol*. 2004:163–89.
47. Ferreira C. Sur l'emploi du bleu de méthylène dans la malaria infantile. *Rev Ther Med Chir*. 1893:488–525.
48. Ehrlich P. Chemotherapeutics: scientific principles, methods, and results. *Lancet*. 1913:445–51.

Supplementary Data

The following additional data are available with the online version of this paper.

- **Additional data file 1** contains 12 large tables on all metabolic flux modes modeled and their changes due to drug action.

- **Additional file 2** is the technical description and a guided tour through all calculations made including a description of the use of all R and PERL scripts.

- **Additional file 3** is a zip file and contains further details and data including all scripts, more detail on the models used as well as detailed results.